Accounts

Synthesis of Carbon Nanotube Composites in Nanochannels of an Anodic Aluminum Oxide Film

Takashi Kyotani,* Bhabendra Kumar Pradhan, and Akira Tomita*

Institute for Chemical Reaction Science, Tohoku University, 2-1-1 Katahira, Sendai 980-8577

(Received April 13, 1999)

A template carbonization technique was applied for synthesizing carbon nanotubes and metal filled nanotubes. An anodic aluminum oxide film that has uniform and straight channels with a diameter at nanometer level was used as a one-dimensional template. The pyrolytic carbon deposition on the channel wall was carried out by exposing the anodic oxide film to hydrocarbon gas at high temperature. The carbon was then liberated from the anodic oxide film by dissolving the alumina template. It was found that the resultant carbon is comprised only of uniform hollow-tubes with open ends. The length and the diameter of the carbon nanotubes are controllable by changing the length and the inner diameter of the channels in the anodic oxide film. By applying this template technique, metal filled uniform carbon nanotubes can also be fabricated. Pt, Ag, and Fe-filled carbon nanotubes were synthesized. If one varies metal the loading and metal reduction methods, various shapes of nano metal compounds can be inserted into the hollow of carbon nanotubes. It should be noted that no metal was observed on the outside walls of the tubes. The metal-filled uniform carbon nanotube thus prepared can be regarded as a novel one-dimensional composite, which has a variety of potential applications.

We developed a template carbonization technique for synthesizing novel carbon materials. This technique utilizes inorganic substances whose opening or pores are controlled at nanometer level. Our first attempt was to prepare ultrathin graphite film from the carbonization of organic polymer in the two-dimensional opening between the lamellae of layered clay such as montmorillonite and taeniolite.[1—5] Then, we applied this template technique to the preparation of new types of porous carbons by using the three-dimensional pores of Y zeolite as space for carbonization of organic polymers and propylene.[6] Our next approach was to prepare one-dimensional carbon by using one-dimensional channels as a template.

Carbon nanotubes are nanometer wide needle-like cylindrical tubes of concentric graphitic carbon. They have attracted much attention due to their potential applications as well as a fundamental interest in their properties. Carbon nanotubes were discovered in 1991 by Iijima[7] when he investigated the material deposited on the cathode for the arc-evaporation synthesis of fullerenes. A short time later, Ebbesen et al. found the optimum arc-evaporation conditions for the production of carbon nanotubes in bulk quantities.[8] Apart from the arc discharge method, several other methods have been proposed: e.g., catalytic pyrolysis of hydrocarbons[9—13] and condensation of a laser-vaporized carbon-catalyst mixture.[14] None of these methods, however, allows the precise control of length, diameter and thickness of carbon nanotubes.

Using uniform and straight channels of anodic oxide film as either a template or a host material, so far many researchers have fabricated a variety of nanomaterials: e.g., magnetic recording media,[15,16] optical devices,[17—20] metal nanohole arrays,[21] and nanotubes or nanowires of polymer, metal and metal oxide.[22—29] No one, however, had tried to use anodic aluminum oxide film to produce carbon nanotubes before we prepared carbon nanotubes by the pyrolytic carbon deposition on the film in 1995.[30] The most striking feature of this method is to allow one to produce monodisperse carbon tubes with uniform length, diameter, and thickness. In the same year, Martin et al. prepared carbon nanotubes by the carbonization of organic polymer in the pores of the film.[31] Three years later, for the production of carbon nanotubes, Martin et al.[32] utilized the pyrolytic deposition method as we did before.[30] We report here how effectively uniform carbon nanotubes can be prepared by the template carbonization technique and how versatile this technique is for the production of novel one-dimensional carbon composites.

1. Formation of Carbon Tubes by Template Technique

When aluminum plate is anodically oxidized in an acid electrolyte, a porous oxide layer is formed on one side of the plate; its porosity consists of an array of parallel and straight channels with a uniform diameter. The cross section of a porous anodic film is illustrated in Fig. 1. The pore size and pore density can be controlled by changing the anodizing

voltage, and the thickness of the oxide film is determined by the anodizing period, i.e. the amount of charge transferred. The attainable minimum pore size depends on the type of electrolyte used for anodic oxidation. It was reported that films with pore size of 10—250 nm, pore densities of 10^{12}—10^{15} m^{-2} and thickness of over 100 μm can be prepared.[33] Although such anodic aluminum oxide films are commercially sold as a membrane filter, only limited standard sizes of pores are available. We prepared anodic aluminum oxide film by anodic oxidation of an electro-polished aluminum plate at a cell voltage of 20 V in 20 wt% sulfuric acid at 0—5 °C for 2 h.[30,34] Following the electrooxidation, the anodic oxide film was separated from the aluminum substrate by reversing the polarity of the cell voltage. Then an impervious layer (referred to as a barrier layer in Fig. 1) was etched by immersing the film in 20 wt% sulfuric acid for 1 h. The diameter and the thickness of this film were 15 mm and 75 μm, respectively, and the diameter of its straight pores was about 30 nm. We used this anodic oxide film together with the commercially available ones as a template for carbon nanotube and metal-filled nanotube production. The following sections describe the details of the template method.

1-1. Carbonization of Organic Polymer in Straight Channels of Anodic Oxide Film. We prepared carbon tubes from organic polymers by using anodic aluminum oxide film.[34] As a film, we employed a commercially available membrane filter 25 mmϕ wide and 60 μm thick (Whatman Ltd., Anodisc 25), whose porosity consists of two types of channels with different diameters (20 and 230 nm). The narrow channels run only 80 nm long from one side of the surface of anodic film and then they merge into wide channels that extend to the other side of the surface. The films (5 or 6 sheets) were impregnated under vacuum with furfuryl alcohol (100 cm^3) together with oxalic acid (0.25 g) as an acid catalyst. The mixture was stirred with the films for 3 d. The polymerization of furfuryl alcohol and its subsequent carbonization were carried out by heating the impregnated films at 900 °C for 3 h under N_2 flow. The resultant carbon-anodic oxide composite films were washed with an excess amount of 46% HF solution at room temperature to dissolve the anodic aluminum oxide template. As a result, carbon was obtained as an insoluble fraction and it was then subjected to SEM (scanning electron microscope) and TEM (transmission electron microscope) observations. For TEM observation, the sample was ground in ethanol and sprayed over a copper grid with plastic substrate (Micro Grid, Oken Shoji Co.). The sample on the grid was observed with a TEM under an accelerating voltage of 200 kV. This simple sampling method was employed for all of our carbon tubes and metal-filled nanotubes.

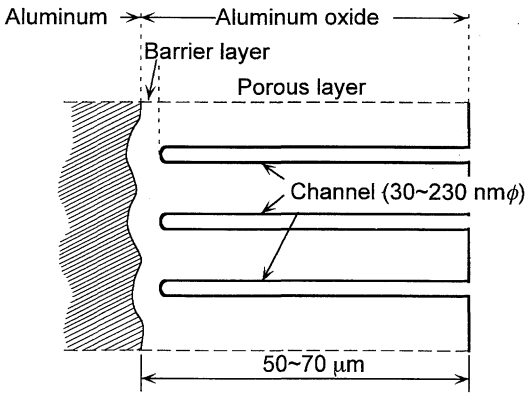

Fig. 1. Structure of anodic aluminum oxide film.

Figures 2a and 2b show SEM and TEM photographs of the resultant carbon sample, respectively. The SEM photograph indicates the formation of tubular carbon, whose diameter is almost equal to the diameter (230 nm) of the wider channels of the anodic oxide film template. Each tube ramifies into several thin tubes near the end. This branch-like structure originates from a similar branching in pore structure of the commercial anodic oxide film near its surface. A more clear view of the structure of the carbon samples is obtained from the TEM photograph (Fig. 2b), which exhibits the presence of voids and knots in the tubes. This is just like bamboo, although we do not have a clear explanation for the formation of such structure. It was confirmed that the carbonization in the one-dimensional channels gives the formation of one-dimensional carbon.

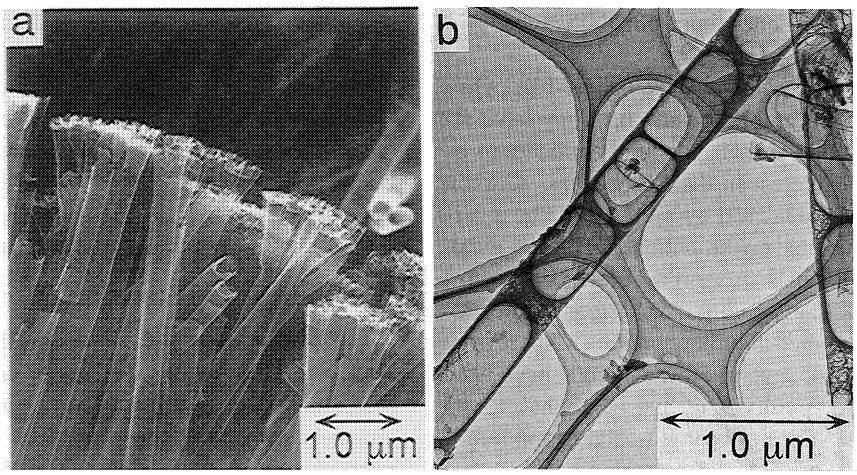

Fig. 2. Photographs of the carbon prepared from poly(furfuryl alcohol): (a) SEM image and (b) TEM image (From Ref. 34).

Martin and coworkers prepared carbon tubes from the carbonization of polyacrylonitrile (PAN) in the channels of anodic oxide film.[31] A commercially available film with a pore diameter of 260 nm was immersed in an aqueous acrylonitrile solution. After addition of initiators, the polymerization was carried out. The resultant PAN/alumina composite film was heat-treated at 250 °C in air and then it was heat-treated at 600 °C under Ar flow for 30 min to carbonize the PAN. Finally, this sample was repeatedly rinsed in 1 M NaOH solution (1 M = 1 mol dm^{-3}) to dissolve the alumina film. The SEM observation of this sample indicated the formation of carbon tubes with about 50 μm long, which corresponds to the thickness of the template film. The inner structure of these tubes was not clear because no TEM images were provided.

1-2. Pyrolytic Carbon Deposition on Anodic Film. In addition to the impregnation method with furfuryl alcohol, we deposited pyrolytic carbon on the inside of the straight channels in the following way.[30,34] This method can produce simple carbon tubes, instead of the bamboo-like tubes. We used two types of anodic aluminum oxide films with different channel diameters (30 and 230 nm). Each anodic oxide film was placed on quartz wool in a vertical quartz reactor (i.d., 20 mmϕ). The reactor temperature was increased to 800 °C under N_2 flow and then propylene gas (2.5% in N_2) was passed through the reactor at a total flow rate of 200 cm^3 (STP) min^{-1}. The thermal decomposition of propylene in the uniform straight channels of the anodic oxide films results in carbon deposition on the channel walls. After a desired period, the reactor was cooled down to room temperature. Then the aluminum oxide template was removed with HF washing as described above and only carbon was left as an insoluble fraction. The formation process of carbon tubes is illustrated in Fig. 3.

Figure 4 shows SEM photographs of the carbon samples from the two types of the films. These photographs reveal that in both cases the samples consist of only cylindrical tubes and their outer diameter is almost the same as the channel diameter of the corresponding anodic oxide film. No other form of carbon was found in the microscopic observation.

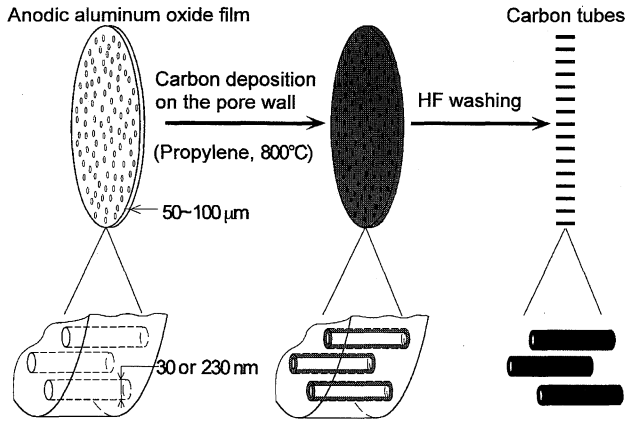

Fig. 3. Schematic drawing of the formation process of carbon tubes (From Ref. 34).

In the SEM photographs with low magnification (Fig. 4c), many bundles of the tubes can be observed and the length of a whole tube in a bundle was almost the same as the thickness of the corresponding template film. Carbon tubes with such uniform diameters and lengths can not be synthesized by the conventional arc-evaporation technique, which generally produces tubes with different sizes. The presence of many bundles in Fig. 4c implies that most of the tubes are connected at the both ends of each tube, because the carbon deposition also took place on the external flat surface of the anodic film. However, some of the tubes were separated from the others during the stirring in the HF solution, as observed in the other pictures. It is noteworthy that the tubes from the anodic oxide film with the smaller channels (Fig. 4b) look transparent under the SEM observation with an acceleration voltage of 15 kV, indicating that the wall thickness of these tubes is very thin.

Figure 5 shows SEM photographs for the carbon tubes under different carbon deposition periods. The photographs, which were taken from the end of the tubes, show the open end structure of these carbon tubes. The other end of the tubes was also such open structure (not shown here). Furthermore, these images clearly demonstrate that the wall thickness of the tubes increases with an increase in the deposition period. The wall thickness could be roughly estimated from the TEM photographs of these tubes (not shown here), where the thickness was in the ranges of 3—5, 40—45, and 60—80 nm for 1-, 6-, and 12 h-deposition, respectively. Although the wall thickness of these 230 nm-tubes kept increasing with the carbon deposition period, such continuous increase in wall thickness was not observed in the case of carbon tubes with an outer-diameter as small as 20 nm. Our recent experiment has revealed that for the tubes with such small diameter the wall thickness was increased to 4 nm by the first 2 h-deposition but further carbon deposition did not change the thickness.

Figure 6 presents a TEM bright field image of the carbon tubes with a diameter of 230 nm and their corresponding electron diffraction patterns. The selected area for each diffraction pattern is indicated by a circle in the images. The pattern (Fig. 6b) exhibits a pair of small but strong arcs for 002, together with weak 10 and 11 diffraction rings. The appearance of the 002 diffraction neither as a ring nor as clear spots, but as a pair of small arcs, indicates some orientation of the 002 planes in the carbon tubes and its poor crystallinity. The pattern (Fig. 6c) was taken from a different area. It is noted that, in the area "b" of Fig. 6a, part of electron beam passed through the tube wall in parallel, but no beam paralleled the wall in the area "c". The 002 arcs as observed in Fig. 6b are not seen in the case of Fig. 6c, where only 10 and 11 rings are observed. This finding suggests that the tube wall consists of cylindrically stacked 002 planes. An electron diffraction pattern similar to Fig. 6b was obtained in the case of the 30 nm-tubes, which are however, too thin to take a diffraction pattern as in Fig. 6c. Accordingly, the observation of 002 lattice image was attempted for these carbon tubes.

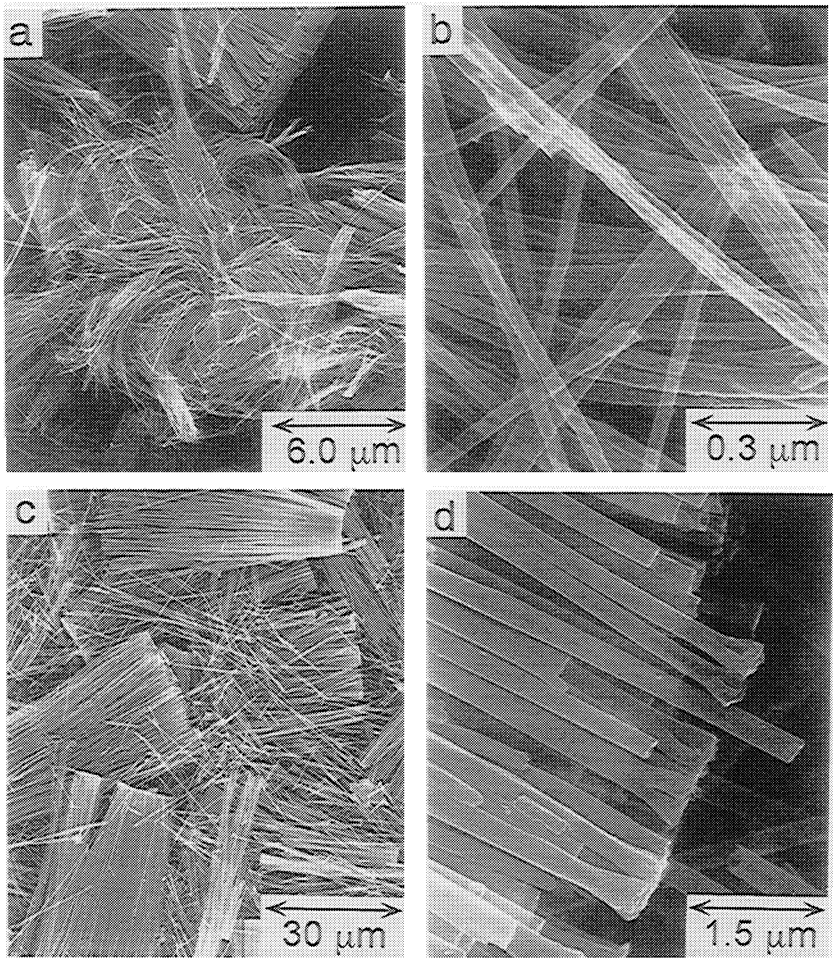

Fig. 4. SEM photographs of the carbon tubes prepared by carbon deposition of propylene: (a) and (b) a carbon deposition period of 1 h on the anodic oxide film with 30 nm-channels; (c) and (d) a period of 12 h on the film with 230 nm-channels (From Ref. 34).

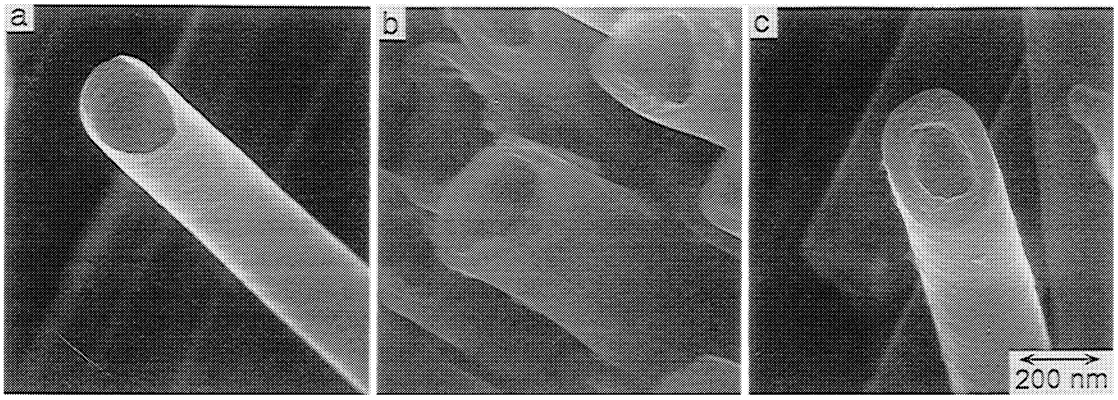

Fig. 5. SEM photographs of the carbon tubes prepared in the anodic oxide film (channel diameter; 230 nm) under different carbon deposition periods: (a) 1 h; (b) 6 h; (c) 12 h (From Ref. 34).

The lattice image for the carbon tubes with a diameter of 30 nm is shown in Fig. 7, where at least four tubes cross each other. The thickness of the walls is about 10 nm and consequently the carbon has a hollow with a diameter as small as 10 nm. Many small lines, which correspond to (002) lattice planes, are observed in the cross section of the walls for each tube. This image demonstrates that the size of most (002) planes is less than 10 nm and they wrinkle to a great extent. This structure is far from graphite, but it should be noted that all the (002) planes are orientated toward the direction of carbon tube axis.

Che et al. recently used the pyrolytic carbon deposition method for the production of carbon tubes.[34] They subjected anodic aluminum oxide template (channel diameter, 200 nm) to either ethylene or pyrene gas stream at 900 °C for 10 min. Then the resultant carbon tubes were removed from the template with HF washing. The carbon tubes thus obtained have almost the same feature as our tubes; i.e., uniform

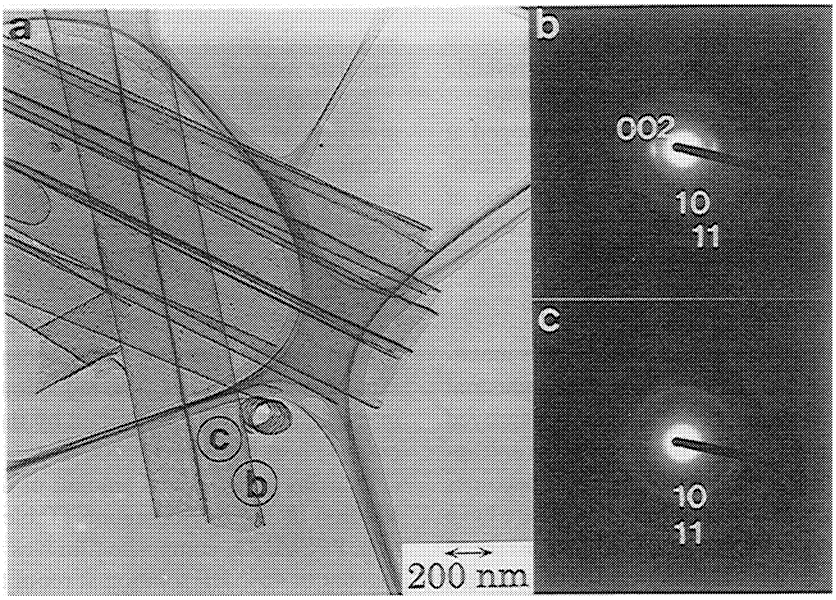

Fig. 6. TEM images of the carbon tubes prepared under a carbon deposition period of 1 h by using the anodic oxide film with 230 nm-channels: (a) bright field image; (b) and (c) electron diffraction patterns from the areas indicated by circles in (a) (From Ref. 30).

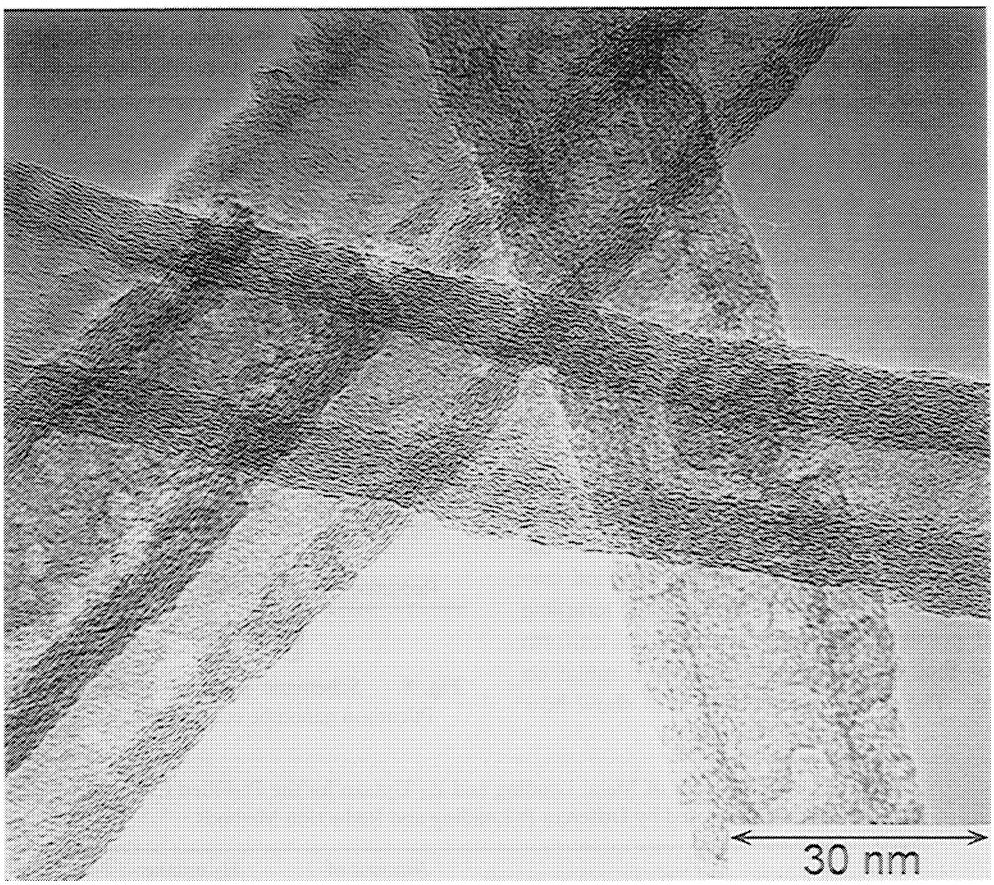

Fig. 7. High resolution TEM image of the carbon tubes prepared in the anodic oxide film with 30 nm-channels under a carbon deposition period of 6 h (From Ref. 34).

carbon tubes with open ends. In addition, using the template coated with Ni catalyst, they synthesized highly crystallized carbon nanofibers at as low a temperature as around 500 °C.

By the template technique using anodic oxide films and pyrolytic carbon deposition, one can prepare monodisperse carbon tubes with uniform diameter and length. Since the length and the inner diameter of the channels in an anodic oxide film can be easily controlled by changing the anodic oxidation period and the current density during the oxidation, it is possible to control the length and the diameter of the car-

bon tubes. Furthermore, by changing the carbon deposition period, the wall thickness of the carbon tubes is controllable to some extent. Another important feature of this template-synthesized carbon tube is that the tubes are not capped at both ends, unlike the carbon nanotubes prepared by the conventional arc discharge method. Thus, the encapsulation of foreign material into the tubes is very easy. The next section describes the metal filling into carbon nanotubes.

2. Metal Filling into Carbon Nanotubes

As reviewed by Freemantle[35] and others,[36,37] the metal-filled carbon nanotubes would have a variety of industrial applications such as catalysts, electronic devices, improved magnetic tape, and biosensors. Thus, the preparation and application of such metal-filled carbon nanotubes now becomes a promising and challenging subject of research. There have been several attempts to insert metal into the tubes prepared by an arc-discharge evaporation technique. These attempts can be classified into the following two methods: one is based on arc-evaporation of a metal-loaded carbon anode and the other one is a two-step method. The former high-temperature method can produce mainly metal carbide-filled nanotubes in a single stage,[38—45] but the yield of filled nanotubes is low, and this method produces impurities such as encapsulated carbon clusters and soot. Higher yield of filled nanotubes can be achieved by the latter method, which consists of the opening of nanotube ends and the inclusion of metal into the opened tubes.[46—51] Early work by Ajayan et al.[46] utilized capillary action to fill molten lead into the nanotubes. A similar approach has been applied by Ugarte et al.[50] and Chen et al.[51] using molten silver nitrate and molten molybdenum oxides, respectively. Green and co-workers[48,49] have developed a wet chemical method, where nanotubes were treated in HNO_3 in the presence of soluble metal salt. As a result, the ends of the nanotubes were opened by the acid treatment and the salt was filled. Thus, the wet chemical method can be applied to a wider variety of materials than the arc-discharge method. A drawback of this chemical method is that some loading on the outer surfaces of nanotubes is unavoidable. Thus, the removal of foreign material from the outside of filled carbon nanotubes is required.[52] On the other hand, the template method makes it possible to prepare metal-filled uniform carbon nanotubes that are completely free from metal on the outer surface. The following sections will show how such metal-filled carbon nanotubes can be prepared by the template method.

2-1. Formation of Pt-Filled Carbon Nanotubes. We prepared Pt-filled carbon nanotubes by several different techniques.[53,54] The anodic aluminum oxide film used in this experiment has a pore size of about 30 nm. The carbon-deposited film was prepared by the CVD of propylene as described above. The film was impregnated under vacuum with an ethanol solution of hexachloroplatinic(IV) acid ($H_2PtCl_6 \cdot 6H_2O$) at room temperature. The mixture was kept for 1 d and then ethanol was evaporated at 80 °C under N_2 flow or under vacuum. The reduction of chloroplatinic acid in the channels was performed by the following two methods; (1) heat treatment at 200 or 500 °C under H_2 flow and (2) stirring in an excess amount of 0.1 M $NaBH_4$ aqueous solution at room temperature (Table 1). After the reduction, $Pt/C/Al_2O_3$ composite film was washed with an excess amount of 46% HF solution at room temperature for 12 h to dissolve the anodic aluminum oxide template. As a result, Pt metal/carbon nanotube composite was obtained as an insoluble fraction. The schematic diagram of the formation process is illustrated in Fig. 8.

Figures 9a and 9b show TEM bright field images with different magnifications for the Pt/carbon tube composite reduced in H_2 at 500 °C. These two images exhibit the presence of uniform carbon nanotubes. Their outer diameter and wall thickness can be estimated from the latter figure to be 30 nm and about 5 nm, respectively. Although some of the tubes are empty, the others are filled with many rod-like materials. The low-magnification TEM image (Fig. 9a) indicates that some of the nanorods are more than 1 μm in length. Their structure was investigated with electron diffraction and with

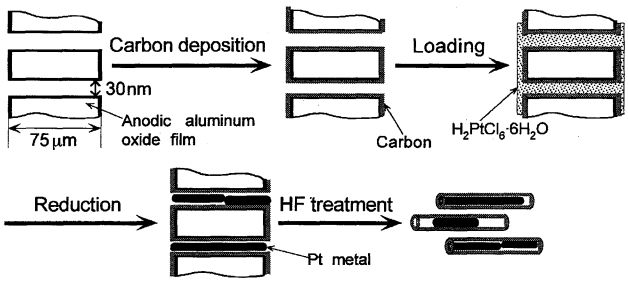

Fig. 8. Schematic diagram of the formation process of Pt/carbon nanotube composites.

Table 1. The Amount of Metal Loading and H_2 Uptake for the Pt-Filled Carbon Nanotubes Prepared by Different Pt Loading and Reduction Methods

Loading method	Reduction method[a)]	Amount of loading (wt%)	H_2 uptake (mol/mol-Pt)
Evaporation to dryness	H_2 at 200 °C	7.3	0.00
Evaporation to dryness	$NaBH_4$ at r.t.	9.7	0.01
Adsorption	$NaBH_4$ at r.t.	5.5	0.02
Ion-exchange	$NaBH_4$ at r.t.	10.4	0.22

a) r.t. stands for room temperature.

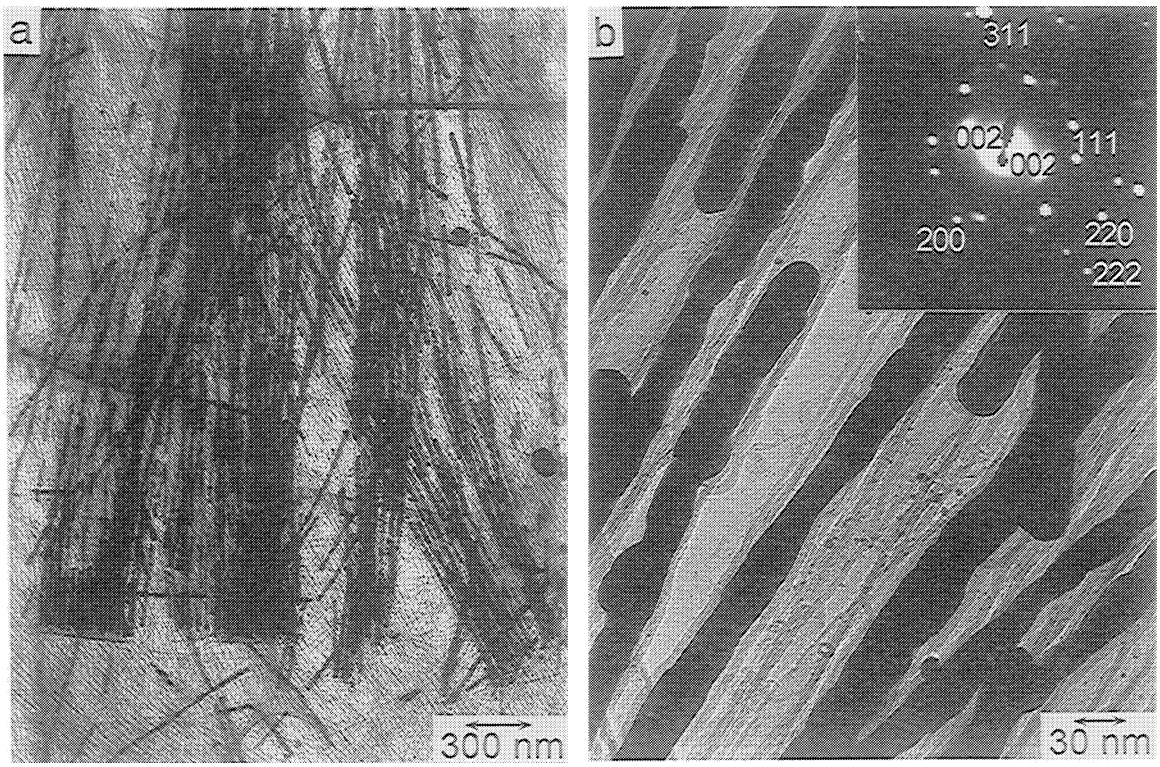

Fig. 9. TEM photographs at different magnifications for the Pt/carbon nanotube composite reduced at 500 °C (a, b). The inset picture shows the electron diffraction pattern taken from the composite in (b). Unless stated otherwise, each inset picture in the following TEM images indicates the diffraction pattern from the sample in the corresponding image (From Ref. 53).

X-ray powder diffraction (XRD). The inset picture in Fig. 9b shows the electron diffraction pattern taken from the composite in this image. The pattern presents the diffraction from Pt metal crystallites as clear spots together with carbon (002) diffraction as a pair of strong arcs. Some of the spots from the fcc structure of Pt metal and carbon (002) arcs are labeled. This pattern confirms the dark materials to be Pt metal. The appearance of the diffraction for Pt as clear spots, not as rings, indicates high crystallinity of Pt nanorods. The small number of these diffraction spots suggests the presence of only a few Pt crystallites in the filled tubes of Fig. 9b. The XRD analysis also confirmed the reduction of chloroplatinic acid to Pt metal. From the peak width of the Pt (111) diffraction, the average crystallite size was calculated to be about 30 nm, which is comparable to the tube diameter. When Pt was reduced with H_2 at 200 °C, we found again a similar rod-like Pt metal in the hollow of carbon nanotubes. Its electron diffraction pattern did not give rings but spots, indicating that the Pt nanorods still keep their high crystallinity even though the reduction temperature was as low as 200 °C.

TEM photographs of the composite reduced by $NaBH_4$ solution at room temperature are displayed in Fig. 10. Like the composite reduced with H_2, Pt metal is observed only in the carbon tube hollows and some tubes look to be completely filled with the metal. There is, however, big difference in microscopic feature between the two types of Pt metals prepared at different temperatures (Figs. 9b and 10b). The Pt metal reduced at room temperature consists of very fine particles with a size of 2—5 nm, which is in good agreement with the calculated value from the XRD analysis. The electron diffraction pattern of the Pt metal gives further information on its structure. The pattern in Fig. 10b exhibits a set of diffraction rings from Pt metal (these rings can be labeled from an inner one as (111), (200), (220), (311) of the fcc Pt metal), together with a pair of carbon (002) arcs. It is noteworthy that the diffraction from Pt metal did not appear as clear spots but as concentric rings, each of which consists of a large number of very small spots. This finding suggests that the metal reduced by $NaBH_4$ solution is comprised of many fine crystallites.

For the above two types of the composites, Pt was loaded by the evaporation to dryness method. The adsorption method was also employed for Pt loading. After the mixture of the film and the chloroplatinic acid solution was stirred at 80 °C for 30 min, the film was filtered out from the solution and then dried. The reduction of Pt was done with $NaBH_4$ solution at room temperature and then the template was removed with HF washing. Figures 11a and 11b show the TEM bright field images with different magnifications for the composite prepared by this loading method. The low magnification image exhibits numerous numbers of very fine foreign particles that are dispersed in the hollows. From the high magnification one, the size of the particles can be estimated to be in the range of 1 to 4 nm. The electron diffraction pattern taken from the tubes in Fig. 11a is shown in its inset picture, which presents very weak rings of Pt (111) and (200) reflections together with strong diffraction from carbon tubes. This finding indicates that the particles observed in

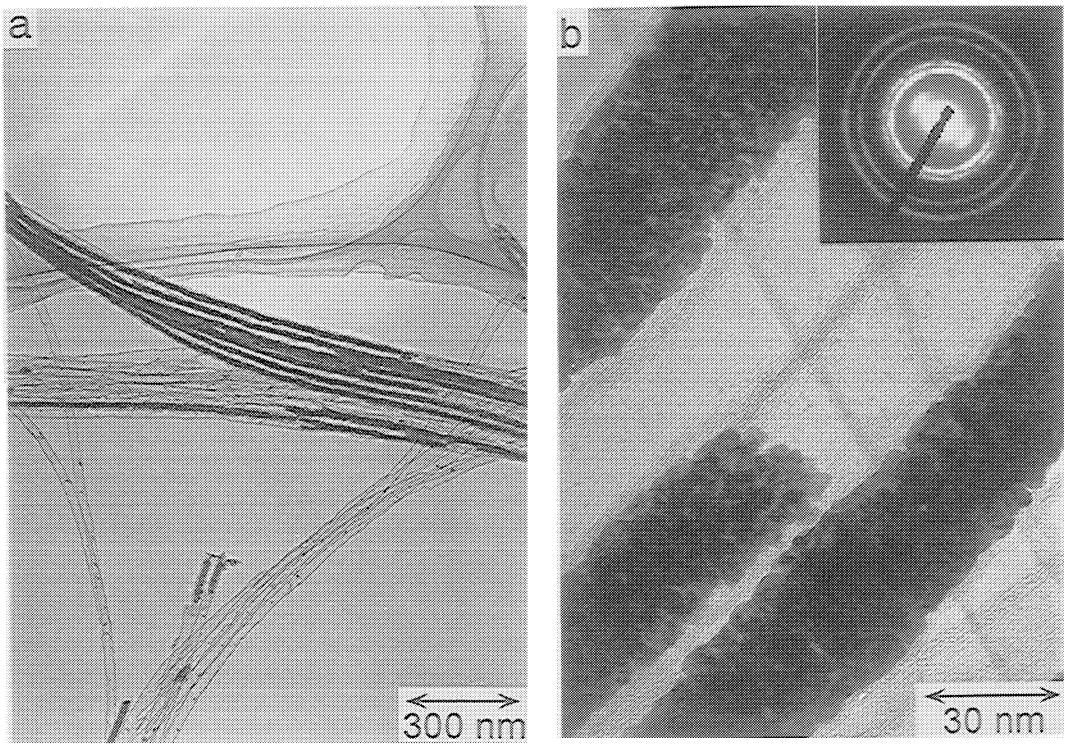

Fig. 10. TEM photographs at different magnifications for the Pt/carbon nanotube composite reduced at room temperature (a, b) (From Ref. 53).

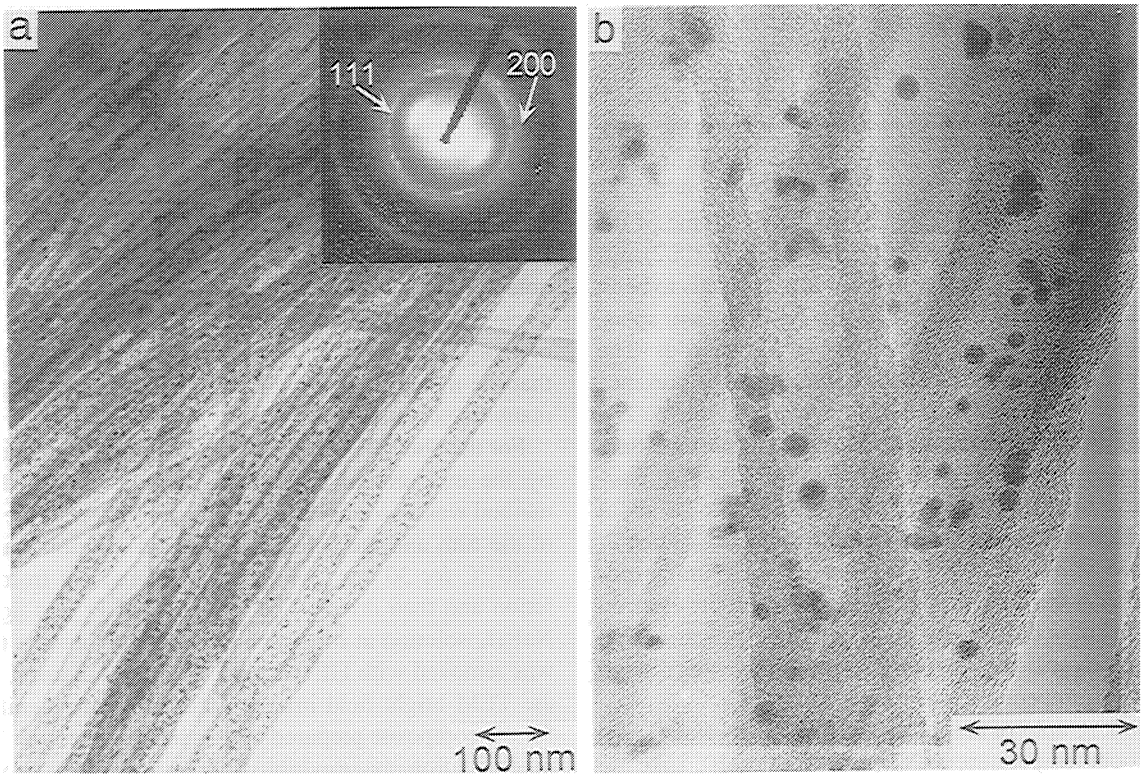

Fig. 11. TEM photographs at different magnifications for the Pt/carbon nanotube composite (a, b). Pt was loaded by the adsorption loading method.

the bright field image (Fig. 11a) are Pt metal. In addition to this adsorption method, we applied the ion-exchange method to Pt loading into carbon nanotubes. The carbon-deposited anodic oxide film was refluxed with concd HNO_3 for 3 h in order to introduce ion-exchangeable sites on the carbon surface. The acid-treated film was ion-exchanged with Pt by soaking the film in an ammoniacal aqueous solution of tetraammineplatinum(II) chloride ($[Pt(NH_3)_4]Cl_2 \cdot nH_2O$) for 1 d.

Then the film was filtered out and washed with deionized water. The reduction of Pt and the subsequent HF washing were done in the same manner as above. The resultant composite was subjected to TEM observation. Its bright field images with different magnifications are shown in Figs. 12a and 12b, where many foreign materials with irregular shapes in the hollows of carbon nanotubes are observed. The foreign materials were identified as Pt metal by the electron diffraction analysis.

For further characterization of Pt metal, the amount of H_2 uptake for some of the samples was determined. The chemisorbed H_2 was measured by a static volumetric method at 20 °C and an equilibrium pressure of about 10 Torr (1 Torr = 133.322 Pa). In order to determine the amount of Pt loading, the supported Pt was extracted by stirring the loaded carbon nanotubes in an aqua regia for 12 h and the amount of Pt extracted was measured by inductively coupled plasma analysis. Table 1 indicates the amounts of Pt loading and H_2 uptake. The very small values of H_2 uptake for the two samples prepared by the evaporation to dryness method can be explained from their morphological features. For these two samples, the Pt metal is present as nanorods wrapped in carbon layers, where it is not expected that H_2 molecules were accessible to most of the Pt atoms. The sample prepared by the adsorption method showed H_2 uptake of only 0.02, which is considerably lower than the case of the ion-exchange method. The amount of H_2 uptake, 0.02, corresponds to spherical particles with a diameter of 32 nm, but the actual size of Pt particles (Fig. 11) is in the range of 1 to 4 nm. At the present moment, we do not have a clear explanation for this discrepancy.

Recently, by using an impregnation method similar to our method, Che et al. prepared Pt/Ru nanoparticle-filled carbon tubes with a diameter of 200 nm.[55] They impregnated carbon-deposited film with a mixture of aqueous solutions of H_2PtCl_6 and $RuCl_3$. Then the metal compounds were reduced by H_2 at 580 °C. The TEM observation of the resultant tubes revealed the presence of Pt/Ru nanoparticles (about 1.6 nm) dispersed on the inner wall of the tubes.

2-2. Formation of Ag-Filled Carbon Nanotubes. Silver filling is also possible by a similar impregnation method.[56] We impregnated the carbon-deposited film with aqueous saturated solution of $AgNO_3$ for 24 h at room temperature and dried it overnight in air at 250 °C. To remove the anodic oxide template after the metal loading, the films were treated with NaOH solution (10 M) at 150 °C for 6—8 h in an autoclave. In this case, HF washing was not applied for alumina removal process because the silver component may be dissolved in HF. Figure 13 shows a TEM image for the Ag/carbon nanotube composites. Although some of the carbon tubes are empty, the others encapsulate many rod-like materials that were observed as dark images. The diffraction pattern presents sharp spots that can be indexed to (111), (200), (220), and (311) reflections from fcc silver metal, with weak arcs and rings from carbon. The presence of the diffraction for Ag as clear spots indicates high crystallinity of Ag nano rods. From the high resolution TEM image of a nano rod (not shown here), we observed regular and straight lattice fringes running in the whole nano rod. The measured *d* spacing of the observed planes of lattice is

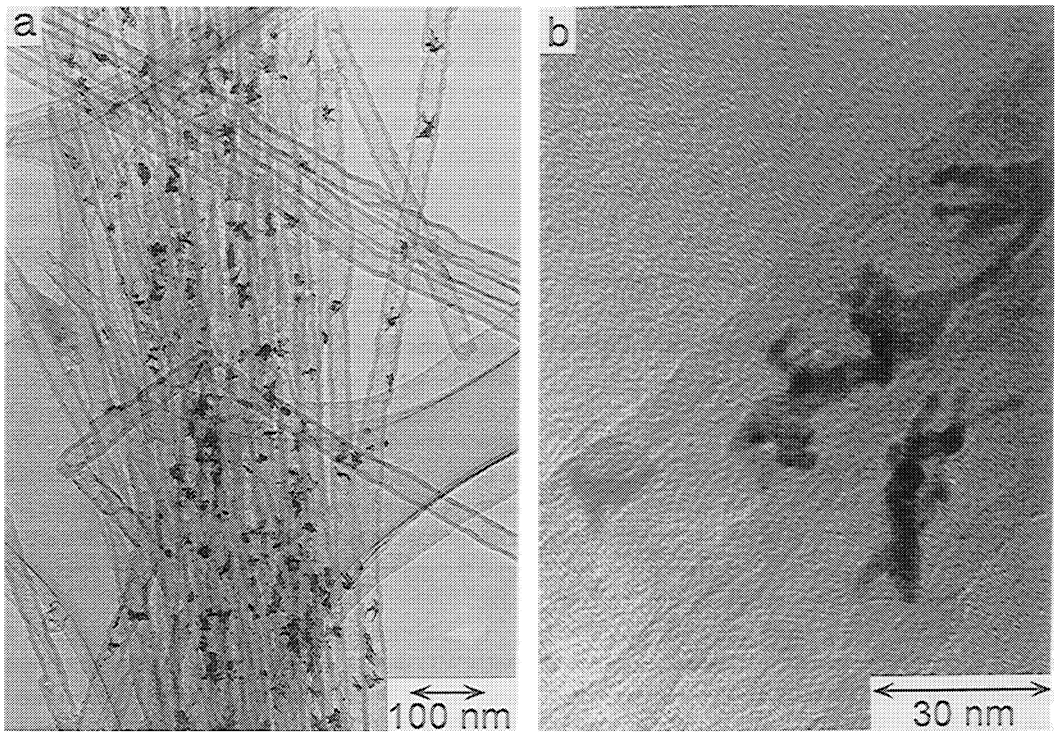

Fig. 12. TEM photographs at different magnifications for the Pt/carbon nanotube composite (a, b). Pt was loaded by the ion-exchange method.

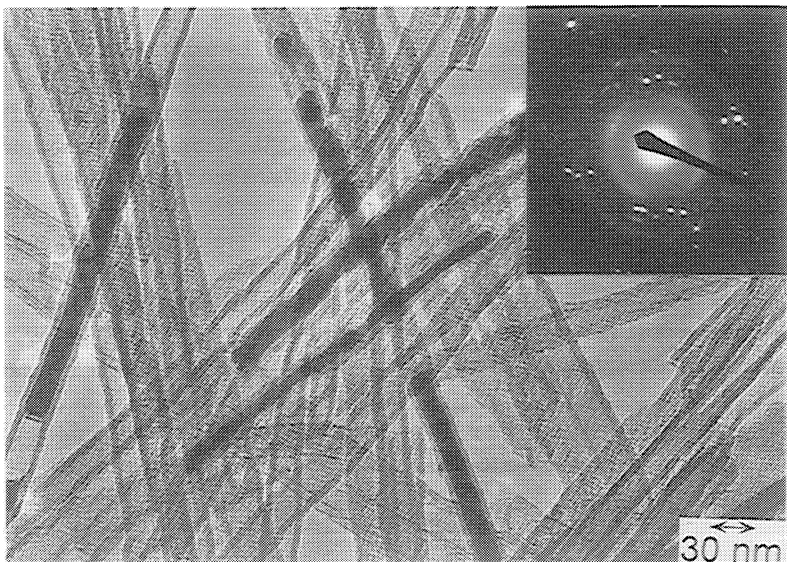

Fig. 13. TEM photograph of the Ag/carbon nanotube composites.

0.250 nm that corresponds to the spacing for (111) plane of fcc silver metal. In order to investigate the formation process of Ag metal, the $AgNO_3$-loaded alumina/carbon composite film was examined by TEM before the heat-treatment at 250 °C. For this purpose, the composite was broken into fine pieces. Some of the nanotubes were separated from the film. Many nanoparticles of $AgNO_3$ were observed in the channels of the tubes. Therefore, the rod-like structure was formed when the composites were treated above the melting point of $AgNO_3$ (212 °C). With the subsequent heat treatment, the salt might be reduced to pure Ag metal.

By applying the template technique, we have succeeded in preparing noble metal-filled uniform carbon nanotubes in which the metal is present as either nanorods or nanoparticles. It should be noted that no metal was observed on the outside wall of the tubes. This is due to the preparation procedure, where the metal precursor was loaded into the carbon-deposited alumina film before the removal of alumina (see Fig. 8). Thus, there is no other space for metal to be loaded except in the channels.

2-3. Inclusion of Crystalline Iron Oxide Nanoparticles in Carbon Nanotubes. We demonstrated that the inclusion of iron oxide nanoparticles into template-synthesized carbon nanotubes was also possible when MOCVD (metal organic chemical vapor deposition) technique was employed.[57] A carbon-deposited film was subjected to MOCVD of ferrocene ($[Fe(C_5H_5)_2]$) in the following manner. Ferrocene was vaporized at 90 or 105 °C (corresponding to the vapor pressure of 0.1 and 0.3 kPa, respectively) and then the vapor was introduced into the film in the quartz reactor with H_2 gas (50% in N_2) at a total flow rate of 100 cm^3(STP) min^{-1}. The feed line was wrapped with heating tapes and maintained at a high temperature to avoid the condensation of ferrocene vapor. The following two series of MOCVD experiments were performed: one is for 3 h with 0.3 kPa of ferrocene pressure at three different temperatures (350, 400, and 500 °C) and the other one for different time periods (0.5, 1, 3, 6, 12, 24 h) with 0.1 kPa at 400 °C. After the MOCVD, the film was treated with 10 M NaOH solution at 150 °C in an autoclave for 6 h in order to remove the template. As a result, metal/carbon nanotube composites were obtained.

Figure 14 shows TEM bright field images at different magnifications for the Fe/carbon tube composite prepared by the MOCVD at 400 °C for 3 h with 0.3 kPa of ferrocene vapor. These images exhibit uniform carbon nanotubes with the outer diameter of 30 nm and the wall thickness of about 5 nm. Although some of the tubes are empty, the others contain many dark particles. It should be noted again that there is no metal deposited outside of the nanotubes. The high magnification image (Fig. 14b) shows that the shape of some particles looks like a cube, implying the high crystallinity of these particles. The inset picture shows the electron diffraction pattern from the composite in Fig. 14a. The pattern presents sharp diffraction spots, which can be indexed to (111), (220), (311), (400), (511), and (440) reflections from cubic magnetite (Fe_3O_4). Together with these spots, arcs and diffused rings from carbon (002), (10), and (11) reflections were observed. The appearance of the diffraction for Fe_3O_4 as clear spots indicates the high crystallinity of Fe_3O_4 nanoparticles. Some of the particles observed in Fig. 14b must be single crystals. The maximum caliper diameter of a hundred particles in the image of Fig. 14a was measured. It was found that their diameters range from 10 to 50 nm with a mean size of 24 nm and the standard deviation of 7 nm. The reason why particles longer than the tube inner diameter (20 nm) were found is that many particles are not spherical and the maximum caliper diameter was used as a measure of size.

In addition to the above experiment at 400 °C, the MOCVD was done at two other different temperatures (350 and 500 °C) for 3 h with 0.3 kPa of ferrocene vapor. Also at 350 and 500 °C, crystalline nanoparticles were formed; their chemical form was identified to be Fe_3O_4 by the corresponding diffraction patterns. It was found that the number

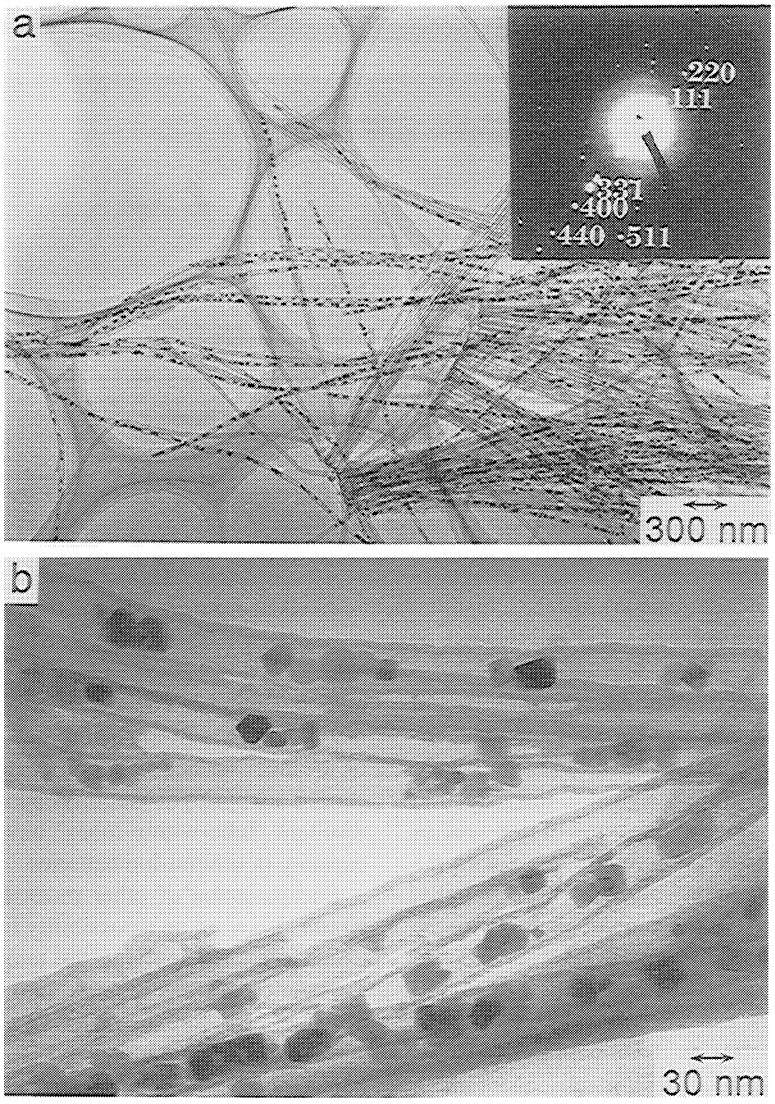

Fig. 14. TEM photographs of the Fe/carbon nanotube composites prepared at a MOCVD temperature of 400 °C for 3 h with ferrocene vapor pressure of 0.3 kPa (a, b) (From Ref. 56).

of nanoparticles and their size increased with MOCVD temperature. Such increases in number and size were reflected in the weight gains of the carbon coated film; the gain was 3.4, 4.1, and 8.3 wt% at 350, 400, and 500 °C, respectively. With assuming all the iron compounds to be Fe_3O_4, we estimated that the iron oxide occupies 8, 10, and 20% of the total volume of the tube hollow for the MOCVD temperature of 350, 400, and 500 °C, respectively. At 500 °C, although a few nanotubes remained empty, most of nanotubes were filled to different degrees and some of them looked completely filled with the metal compound. The fraction of empty tubes in the case of MOCVD at 500 °C was quite low in comparison with the cases of 350 and 400 °C.

The effect of MOCVD period was also investigated at 400 °C with 0.1 kPa of ferrocene vapor. When the MOCVD was carried out only for a short period as 0.5 h, most of the nanotubes were found to be empty. Only a few of them contained Fe_3O_4 nanoparticles, whose mean size was 5 nm with a standard deviation of 1 nm. With increasing MOCVD period, the size of nanoparticles gradually increased: 16±5, 20±9, and 22±7 nm at 1, 6, and 12 h-MOCVD, respectively. The weight gain at the 12 h-MOCVD was 9.3%, which corresponds to 22% filling of the total volume of the tube hollows.

The iron oxide was likely to be formed when the iron loaded carbon/alumina film was exposed to air and/or when the film was treated with an alkaline solution. In order to clarify this issue, we characterized the iron-containing carbon nanotubes before the alkali treatment. After the MOCVD experiment, the iron-loaded carbon/Al_2O_3 film was taken out to the ambient air and broken into fine pieces. The TEM observation showed that some nanotubes protruded from several broken Al_2O_3 pieces and also some of the nanotubes were isolated from the film. Figure 15 exhibits a TEM image of such an isolated carbon nanotube containing nanoparticles. Most of these particles comprise a dark core surrounded with some other type of substance, whereas such a dual structure was not observed in the case of very small particles. The corresponding electron diffraction pattern (the inset picture) presents sharp clear spots which were identified as the re-

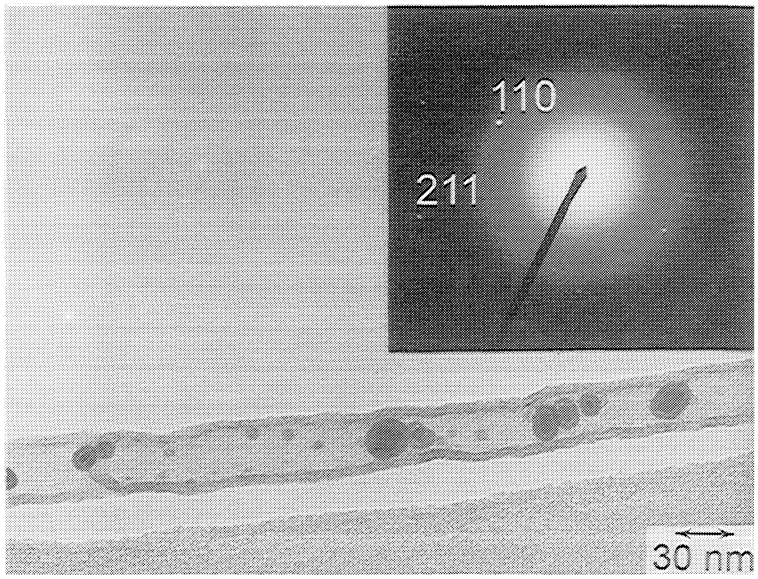

Fig. 15. TEM photograph of the Fe/carbon nanotube composites before the alkali treatment (MOCVD temperature, 400 °C; MOCVD period, 24 h; ferrocene vapor pressure, 0.1 kPa) (From Ref. 56).

flection from α-Fe (the spots can be indexed to (110) and (211)). The diffused rings were from carbon nanotube. Together with these clear spots, several very weak spots were observed. All of these spots were assigned to the reflection from Fe_3O_4. Taking the presence of two types of iron species (α-Fe and Fe_3O_4) into consideration, one may explain the formation of a dual structure in the following way. Initially, iron metal particles deposited in the nanotube hollow by the MOCVD under H_2 flow. When these particles were exposed to air, their surface was oxidized to iron oxide (Fe_3O_4) to leave the metal (α-Fe) in the particle core, while very small metal particles were completely oxidized with the air exposure. Upon further exposure to air and/or subsequent alkali treatment, the remaining metal core was oxidized to Fe_3O_4 as observed in Fig. 14.

In this work, we demonstrated the encapsulation of crystalline Fe_3O_4 nanoparticles into the uniform carbon nanotubes by the MOCVD technique using ferrocene. The size and number of such nanoparticles can easily be controlled by changing the MOCVD temperature or period. Under a certain condition, Fe_3O_4 nanocrystals could be introduced into all of the nanotubes, and more than 20% of the total volume of the tube hollow was filled with the nanoparticles.

3. Potential Applications of Template-Synthesized Carbon Nanotubes

As demonstrated in this paper, the template technique using anodic oxide films can control the length, diameter, and thickness of carbon tubes and can produce monodisperse carbon nanotubes. The carbon nanotubes prepared by this method have rather low crystallinity. This makes the application as nanoelectrodevices or "the ultimate carbon fibers" difficult, because defect-free structure is required for these purposes. However, the application to electrochemical devices such as lithium-ion batteries is not so difficult. The group of Martin demonstrates that the template-synthesized carbon nanotubes could be used as high performance anode material in lithium-ion batteries.[55] They loaded iron particles on the inner surface of carbon-coated channels and then again carried out pyrolytic carbon deposition. It was found that the resultant "tube-within-tubes" have a high Li^+ intercalation capacity in lithium-ion batteries.

Encapsulation of other materials into carbon nanotubes would also open up a possibility for the applications to electrodevices. By applying the template method, perfect encapsulation of other material into carbon nanotubes became possible. No foreign material was observed on the outer surface of carbon nanotubes. The metal-filled uniform carbon nanotubes thus prepared can be regarded as a novel one-dimensional composite, which could have a variety of potential applications: e.g., novel catalysts for noble metal filled nanotubes and magnetic nanodevices for Fe_3O_4-filled nanotubes. Furthermore, the template method enables selective chemical modification onto the inner surfaces of carbon nanotubes.[58] Since only the inner wall of carbon nanotubes is exposed to the atmosphere before the removal of alumina template, it is possible to modify only the inner surface. With this technique, carbon nanotubes whose outer and inner surfaces have different properties can be prepared, and unique adsorption behaviors and unique electrical properties can be expected from such carbon nanotubes with hetero-properties.

This work would not have been possible without the great efforts of the following highly motivated students: Li-fu Tsai, Tomoko Toba, and Masayuki Kawashima. We also thank the High Voltage Electron Microscope Laboratory of Tohoku University for electron microscopical analysis. This work was partly supported by the Ministry of Education, Science, Sports and Culture, Grant-in-Aid for Scientific Research on Priority Areas, No. 288 Carbon Alloys and by the Mitsubishi Foundation.

References

1 T. Kyotani, N. Sonobe, and A. Tomita, *Nature*, **331**, 331 (1988).

2 N. Sonobe, T. Kyotani, Y. Hishiyama, M. Shiraishi, and A. Tomita, *J. Phys. Chem.*, **92**, 7029 (1988).

3 N. Sonobe, T. Kyotani, and A. Tomita, *Carbon*, **29**, 61 (1991).

4 T. Kyotani, H. Yamada, N. Sonobe, and A. Tomita, *Carbon*, **32**, 627 (1994).

5 T. Kyotani, T. Mori, and A. Tomita, *Chem. Mater.*, **6**, 2138 (1994).

6 T. Kyotani, T. Nagai, S. Inoue, and A. Tomita, *Chem. Mater.*, **9**, 609 (1997).

7 S. Iijima, *Nature*, **354**, 56 (1991).

8 T. W. Ebbesen and P. M. Ajayan, *Nature*, **358**, 220 (1992).

9 M. Endo, K. Takeuchi, S. Igarashi, K. Kobori, M. Shiraishi, and H. W. Kroto, *J. Phys. Chem. Solids*, **54**, 1841 (1993).

10 M. Endo, K. Takeuchi, K. Kobori, K. Takahashi, H. W. Kroto, and A. Sarka, *Carbon*, **33**, 873 (1995).

11 V. Ivanov, J. B. Nagy, P. Lambin, A. Lucas, X. B. Zhang, X. F. Zhang, D. Bernaerts, G. van Tendeloo, S. Amelinkx, and J. van Landuyt, *Chem. Phys. Lett.*, **223**, 329 (1994).

12 W. Z. Li, S. S. Xie, L. X. Qian, B. H. Chang, B. S. Zou, W. Y. Zhou, R. A. Zhao, and G. Wang, *Science*, **274**, 1701 (1996).

13 M. Terrones, N. Grobert, J. Olivares, J. P. Zhang, H. Terrones, K. Kordatos, W. K. Hsu, J. P. Hare, P. D. Townsend, K. Prassides, A. K. Cheetham, H. W. Kroto, and D. R. M. Walton, *Nature*, **388**, 52 (1997).

14 A. Thess, R. Lee, P. Nikolaev, H. Dai, P. Petit, J. Robert, C. Xu, Y. H. Lee, S. G. Kim, A. G. Rinzler, D. T. Colbert, G. E. Scuseria, D. Tománek, J. E. Fischer, and R. E. Smalley, *Science*, **273**, 483 (1996).

15 S. Kawai and R. Ueda, *J. Electrochem. Soc.*, **122**, 32 (1975).

16 D. AlMawlawi, N. Coombs, and M. Moskovits, *J. Appl. Phys.*, **70**, 4421 (1991).

17 C. A. Foss, Jr., G. L. Hornyak, J. A. Stockert, and C. R. Martin, *J. Phys. Chem.*, **96**, 7497 (1992).

18 C. A. Foss, Jr., G. L. Hornyak, J. A. Stockert, and C. R. Martin, *Adv. Mater.*, **5**, 135 (1993).

19 C. A. Foss, Jr., G. L. Hornyak, J. A. Stockert, and C. R. Martin, *J. Phys. Chem.*, **98**, 2963 (1994).

20 G. L. Hornyak, C. J. Patrissi, and C. R. Martin, *J. Phys. Chem. B*, **101**, 1548 (1997).

21 H. Masuda and K. Fukuda, *Science*, **268**, 1466 (1995).

22 P. Hoyer, N. Baba, and H. Masuda, *Appl. Phys. Lett.*, **66**, 2700 (1995).

23 P. Hoyer, *Langmuir*, **12**, 1411 (1996).

24 B. B. Lakshmi, P. K. Dorhout, and C. R. Martin, *Chem. Mater.*, **9**, 857 (1997).

25 C. J. Brumlik and C. R. Martin, *J. Am. Chem. Soc.*, **113**, 3174 (1991).

26 W. Liang and C. R. Martin, *J. Am. Chem. Soc.*, **112**, 9666 (1990).

27 D. N. Davydov, J. Haruyama, D. Routkevitch, B. W. Statt, D. Ellis, M. Moskovits, and J. M. Xu, *Phys. Rev. B*, **57**, 13550 (1998).

28 F. Schlottig, M. Textor, N. D. Spencer, K. Sekinger, U. Shnaut, and J. -F. Paulet, *Fresenius J. Anal. Chem.*, **361**, 684 (1998).

29 D. Routkevitch, T. Bigioni, M. Moskovits, and J. M. Xu, *J. Phys. Chem.*, **100**, 14037 (1996).

30 T. Kyotani, L. Tsai, and A. Tomita, *Chem. Mater.*, **7**, 1427 (1995).

31 R. V. Parthasarathy, K. L. N. Phani, and C. R. Martin, *Adv. Mater.*, **7**, 896 (1995).

32 G. Che, B. B. Lakshmi, C. R. Martin, and E. R. Fisher, *Chem. Mater.*, **10**, 260 (1998).

33 R. C. Furneaux, W. R. Rigby, and A. P. Davidson, *Nature*, **337**, 147 (1989).

34 T. Kyotani, L. Tsai, and A. Tomita, *Chem. Mater.*, **8**, 2109 (1996).

35 M. Freemantle, *Chem. Eng. News*, **74**, 62 (1996).

36 J. Cook, J. Sloan, and M. L. H. Green, *Chem. Ind.*, **16**, 600 (1996).

37 T. W. Ebbesen, *Phys. Today*, **49**, 26 (1996).

38 M. Liu and J. M. Cowley, *Carbon*, **33**, 749 (1995).

39 Y. Murakami, T. Shibata, K. Okuyama, T. Arai, H. Suematsu, and Y. Yoshida, *Phys. Chem. Solids*, **54**, 1861 (1993).

40 S. Subramoney, R. S. Ruoff, D. C. Lorents, B. Chan, R. Malhotra, M. J. Dyer, and K. Parvin, *Carbon*, **32**, 507 (1994).

41 Y. Saito, T. Yashikawa, M. Okuda, N. Fujimoto, K. Sumiyama, K. Suzuki, A. Kasuya, and Y. Nishina, *J. Phys. Chem. Solids*, **54**, 1849 (1994).

42 C. Guerret-Piecourt, Y. Le Bouar, A. Loiseau, and H. Pascard, *Nature*, **372**, 761 (1994).

43 A. A. Setlur, J. M. Lauerhaas, J. Y. Dai, and R. P. Chang, *Appl. Phys. Lett.*, **69**, 345 (1996).

44 A. Loiseau and H. Pascard, *Chem. Phys. Lett.*, **256**, 246 (1996).

45 J. Y. Dai, J. M. Lauerhaas, A. A. Setlur, and R. P. H. Chang, *Chem. Phys. Lett.*, **258**, 547 (1996).

46 P. M. Ajayan and S. Iijima, *Nature*, **361**, 333 (1993).

47 B. C. Satishkumar, A. Govindaraj, J. Mofokeng, G. N. Subbanna, and C. N. R. Rao, *J. Phys. B*, **66**, 839 (1994).

48 S. C. Tsang, Y. K. Chen, P. J. F. Harris, and M. L. H. Green, *Nature*, **372**, 159 (1994).

49 A. Chu, J. Cook, R. J. R. Heeson, J. L. Hutchison, M. L. H. Green, and J. Sloan, *Chem. Mater.*, **8**, 2571 (1996).

50 U. Ugarte, A. Châtelain, and W. A. de Heer, *Science*, **274**, 1897 (1996).

51 Y. K. Chen, M. L. H. Green, and S. C. Tsang, *J. Chem. Soc., Chem. Commun.*, **1996**, 2489.

52 J. Cook, J. Sloan, R. J. R. Heesom, and M. L. H. Green, *J. Chem. Soc., Chem. Commun.*, **1996**, 2673.

53 T. Kyotani, L. Tsai, and A. Tomita, *J. Chem. Soc., Chem. Commun.*, **1997**, 701.

54 M. Kawashima, T. Kyotani, and A. Tomita, "Preprint of 24th Annual Meeting," The Carbon Society of Japan, Matsuyama, 1997, Abstr., p. 320.

55 G. Che, B. B. Lakshmi, E. R. Fisher, and C. R. Martin, *Nature*, **393**, 346 (1998).

56 B. K. Pradhan, T. Kyotani, and A. Tomita, "Extended Abstracts, International Symposium on Carbon, Science and Technology for New Carbons," Tokyo, 1998, Abstr., p. 132.

57 B. K. Pradhan, T. Toba, T. Kyotani, and A. Tomita, *Chem. Mater.*, **10**, 2510 (1998).

58 Y. Hattori, Y. Watanabe, S. Kawasaki, F. Okino, B. K. Pradhan, T. Kyotani, A. Tomita, and H. Touhara, *Carbon.*, **37**, 1033 (1999).

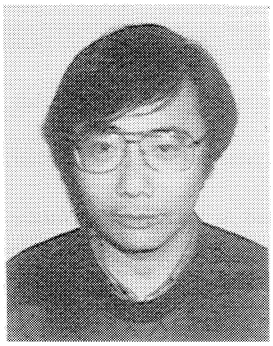

Takashi Kyotani was born in 1954 in Osaka, Japan. He received his B. Eng. degree in 1977 from Osaka City University, M. Eng. in 1979 and D. Eng. in 1983 from Tohoku University. He joined the Research Institute of Non-Aqueous Solutions (currently, Institute for Chemical Reaction Science), Tohoku University, as a research associate in 1982. He was promoted to lecturer in 1990 and to associated professor in 1991 of the same Institute. His current interests include the production of new carbon materials and the analysis of coal conversion reactions.

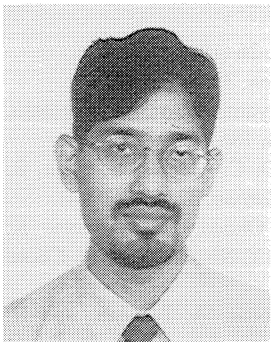

Bhabendra Kumar Pradhan was born in 1969 at Bhawanipatana in Orissa, India. He received his B. Sc. degree in 1990, M. Sc. degree in 1992 from Sambalpur University, and Ph. D. in 1997 from IIT Delhi, India. After his graduation, he joined the Institute for Chemical Reaction Science, Tohoku University as lecturer. Now he is a research associate at the Department of Energy and Geo-Environmental Engineering, Penn State University, USA. His current interests include new carbon materials, surface properties of carbon materials, and use of carbon materials for pollution control.

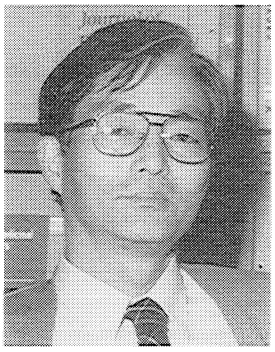

Akira Tomita was born in 1940 in Osaka, Japan. He received his B. Eng. degree in 1963 from Tokyo University, M. Eng. in 1965 and D. Eng. in 1968 from the same University. He joined the Research Institute of Non-Aqueous Solutions (currently, Institute for Chemical Reaction Science), Tohoku University as a research associate in 1968. He was promoted to associate professor in 1977 and to full professor in 1984 of the same Institute. His current interests include carbon materials, coal conversion, and chemistry for environmental protection.